

Influence of the anisotropy on the magneto-acoustic response of magnetic surface acoustic wave resonators

Yawei Lu(鲁亚巍), Wenbin Hu(胡文彬), Wan Liu(刘婉), Feiming Bai(白飞明)

Citation: Chin. Phys. B . 2020, 29(6): 067504 . **doi:** 10.1088/1674-1056/ab8375
Journal homepage: http://cpb.iphy.ac.cn; http://iopscience.iop.org/cpb

What follows is a list of articles you may be interested in

Three- and two-dimensional calculations for the interface anisotropy dependence of magnetic properties of exchange-spring $Nd_2Fe_{14}B$/*α*-Fe multilayers with out-of-plane easy axes

Qian Zhao(赵倩), Xin-Xin He(何鑫鑫), Francois-Jacques Morvan(李文瀚), Guo-Ping Zhao(赵国平), Zhu-Bai Li(李柱柏)
Chin. Phys. B . 2020, 29(3): 037501 . **doi:** 10.1088/1674-1056/ab69e9

Two-dimensional XSe_2 (*X*=Mn, V) based magnetic tunneling junctions with high Curie temperature

Longfei Pan(潘龙飞), Hongyu Wen(文宏玉), Le Huang(黄乐), Long Chen(陈龙), Hui-Xiong Deng(邓惠雄), Jian-Bai Xia(夏建白), Zhongming Wei(魏钟鸣)
Chin. Phys. B . 2019, 28(10): 107504 . **doi:** 10.1088/1674-1056/ab3e45

Realization of artificial skyrmion in CoCrPt/NiFe bilayers

Yi Liu(刘益), Yong-Ming Luo(骆泳铭), Zheng-Hong Qian(钱正洪), Jian-Guo Zhu(朱建国)
Chin. Phys. B . 2018, 27(12): 127503 . **doi:** 10.1088/1674-1056/27/12/127503

Strong anti-strain capacity of CoFeB/MgO interface on electronic structure and state coupling

Fei Guo(郭飞), Yaping Wu(吴雅苹), Zhiming Wu(吴志明), Ting Chen(陈婷), Heng Li(李恒), Chunmiao Zhang(张纯淼), Mingming Fu(付明明), Yihong Lu(卢奕宏), Junyong Kang(康俊勇)
Chin. Phys. B . 2018, 27(1): 017502 . **doi:** 10.1088/1674-1056/27/1/017502

Effect of exchange coupling on magnetic property in Sm-Co/*α*-Fe layered system

C X Sang(桑成祥), G P Zhao(赵国平), W X Xia(夏卫星), X L Wan(万秀琳), F J Morvan, X C Zhang(张溪超), L H Xie(谢林华), J Zhang(张健), J Du(杜娟), A R Yan(闫阿儒), P Liu(刘平)
Chin. Phys. B . 2016, 25(3): 037501 . **doi:** 10.1088/1674-1056/25/3/037501

Influence of the anisotropy on the magneto-acoustic response of magnetic surface acoustic wave resonators*

Yawei Lu(鲁亚巍), Wenbin Hu(胡文彬), Wan Liu(刘婉), and Feiming Bai(白飞明)†

State Key Laboratory of Electronic Thin Film and Integrated Devices, University of Electronic Science and Technology, Chengdu 610054, *China*

(Received 4 February 2020; revised manuscript received 24 March 2020; accepted manuscript online 26 March 2020)

One-port magnetic surface acoustic wave (MSAW) resonators are fabricated by stacking multilayered $(FeCoSiB/SiO_2)_n$ films directly on top of interdigital electrodes. It is shown that the magneto-acoustic response of the MSAW resonators critically depends the hysteresis of ΔE effect. For the magnetic multilayer without induced magnetic anisotropy, the resonance frequency (f_R) exhibits a butterfly-like dependence on the external field, therefore, enabling bipolar detection of magnetic field smaller than its coercive field. However, for the magnetic multilayers with induced magnetic anisotropy, butterfly-like or loop-like f_R–H curves are measured along the interdigtial electrode fingers or the SAW propagation direction, which can be attributed to the competition between the magnetic field-induced anisotropy and the stress-induced or shape anisotropy.

Keywords: surface acoustic wave, magnetic field sensor, magnetoelastic property

PACS: 75.70.Cn, 68.65.−k, 07.07.Df, 77.65.Dq **DOI:** 10.1088/1674-1056/ab8375

1. Introduction

In the past decades, considerable efforts have been devoted to investigate the magnetostrictive-elastic-piezoelectric interaction for magnetic field sensor applications.[1–3] Giant magnetoelectric (ME) coefficients have been reported in both bulk laminates, such as PZT/Terfenol-D,[4,5] PMNT/Terfenol-D,[6] PMNT/Metglas,[7,8] etc., and AlN/FeCoSiB bilayered films.[9–11] Ultra-high sensitivity (pico-Tesla range) has been demonstrated by employing the mechanical resonance enhancement effect.[8] However, the sensitivity becomes poor at low frequency, mainly because of the $1/f$ noise (f is the frequency).[12,13]

This intrinsic difficulty can be overcome by introducing the ΔE effect, i.e., the variation of Young's modulus under a magnetic field.[14,15] The ΔE-effect has been used to detune cantilever,[16–18] surface acoustic waves (SAWs)[19–24] or bulk acoustic wave (BAW) devices[25,26] coated with a magnetic material. Taking magnetic SAW resonators and delay lines for example, the phase velocity of the piezoelectric substrate becomes highly dispersive upon coating a magnetic layer onto[21,24] or in-between[20,23] the interdigital electrodes (IDTs), or replacing the nonmagnetic IDTs with magnetic ones.[19,22] Recently, an ultrahigh DC magnetic field sensitivity of 2.8 Hz/nT and a limit of detection of 800 pT were reported by Sun's group using a contour-mode resonator at room temperature.[26] Additionally, a very low magnetic noise level of 100 pT/ Hz and a bandwidth of 50 kHz have been achieved by Kiel University researchers using a Love-mode delay line.[27]

Despite these remarkable advances, the hysteresis of the ΔE effect on the magnetoacoustic response of MSAW resonators was largely ignored, which is rooted in the magnetoelastic properties, i.e., the larger the magnetostrictive coefficient the larger the ΔE effect.[15] In addition, coupled to dynamic magnetic oscillations, SAWs can be also used to assist the magnetic domain motion, therefore, affecting the static hysteresis of the ΔE effect.[28,29] In current work, we have fabricated one-port MSAW resonators composing multilayered $(FeCoSiB/SiO_2)_n$ stacks directly on top of interdigital electrodes. Similar structure was reported by Liu *et al.*[24] to achieve self-biased magnetic sensors, however, our attention is given to the hysteresis of the ΔE effect. The influence of the magnetic field-induced anisotropy, the stress-induced anisotropy, and the shape anisotropy on the magnetoacoustic properties was studied in details. Hysteresis-loop-like and butterfly-like resonance frequency versus applied field (f_R–H) curves were obtained, which enable the detection of not only the bipolar magnetic field, but also the vector magnetic fields.

2. Experimental methods

$[FeCoSiB\ (160\ nm)/SiO_2\ (10\ nm)]_n$ multilayered films were deposited by magnetron sputtering using a $(Fe_{90}Co_{10})_{78}Si_{12}B_{10}$ target. FeCoSiB was selected in this study due to its large saturation magnetostrictive coefficient ($\lambda_s \sim 60$ ppm) and ΔE effect (30%).[15] The multilayered structure was employed to suppress the perpendicular

*Project supported by the National Natural Science Foundation of China (Grant No. 61871081) and the National Key Scientific Instrument and Equipment Development Project of China (Grant No. 51827802).

†Corresponding author. E-mail: fmbai@uestc.edu.cn

© 2020 Chinese Physical Society and IOP Publishing Ltd

anisotropy.[30] A fixed 200 Oe biasing field was applied *in situ* during deposition to induce magnetic anisotropy. Figure 1(a) shows the *M*–*H* curves of the deposited [FeCoSiB/SiO_2]$_3$ film on a Si wafer along the easy and hard axes. The large remanent ratio and the low coercivity of 2.3 Oe suggest the excellent soft magnetic properties of the film. Figure 1(b) presents the complex permeability spectra of the multilayered film measured by a shorted microstrip perturbation method.[31] The real permeability μ' is ~ 600 and the ferromagnetic resonance frequency is 1.5 GHz. Since the magnetic field dependent stiffness and the magneto-elastic coupling are proportional to μ', a large μ' is desired for a highly sensitive MSAW resonator.

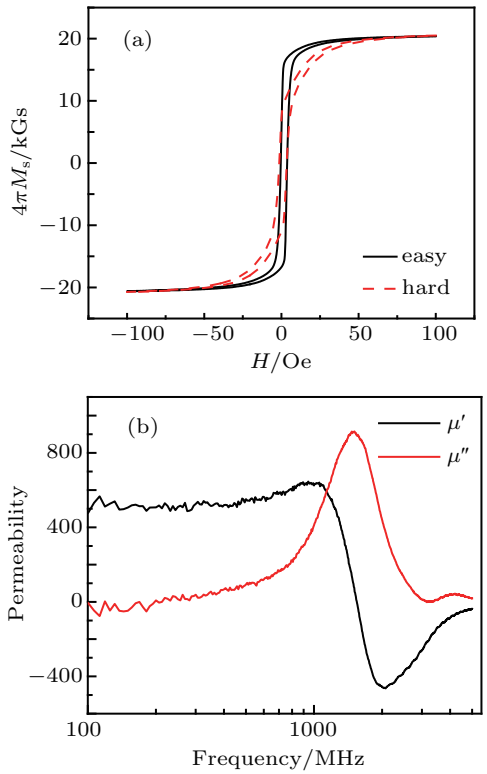


Fig. 1. (a) The *M*–*H* curves along the easy and hard axes, and (b) the complex permeability spectra of the multilayered [FeCoSiB/SiO_2]$_3$ film on a Si wafer.

One-port Rayleigh-mode SAW resonators were fabricated on ST-cut quartz using 100-nm-thick aluminum interdigital electrodes, as shown in Fig. 2. The detailed structure parameters are listed in Table 1. [FeCoSiB(160 nm) /SiO_2 (10 nm)]$_n$ ($n = 1, 3, 5$) multilayered films were then deposited on top of the IDTs. A 30-nm-thick SiO_2 was used as the insulator in-between the magnetic multilayer and the IDTs. Notice that the metallization ratio is 0.75, which allows the deposition of a relatively smooth magnetic multilayer, as shown by the cross sectional SEM image in Fig. 2(c). In order to investigate the effect of magnetic anisotropy on the acoustic response, we have prepared three MSAW resonators with no induced magnetic anisotropy (MSAW-A), induced anisotropy parallel to the SAW propagation direction (MSAW-B) and parallel to the fingers of the IDTs (MSAW-C).

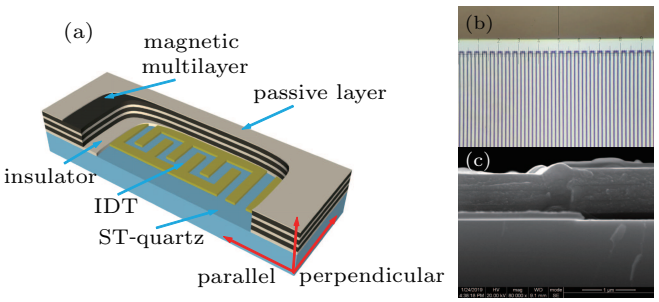


Fig. 2. (a) Schematic illustration of the structure of magnetic SAW resonator, (b) the optical image of IDTs, and (c) the cross sectional SEM image of the MSAW resonator.

The MSAW resonator was then bonded to a printed circuit board (PCB) and connected to a 50 Ω buffer. The *S*-parameter was tested using a vector network analyzer (Agilent N5230 A). The magnetic field employed for testing was generated by a set of Helmholtz coils, and supplied by a Keithley 2400 source meter. Magnetic field calibration was done by using a Lakeshore 475 Gaussmeter. All the measurements were controlled by a programmed Labview software.

Table 1. Device design of the one-port MSAW resonators.

Line width	3.75 μm
Wavelength	10 μm
Number of IDT finger pairs, N_I	100
Aperture/IDT periodicity	0.25
Reflection grid number	500
Distance of reflection grid and IDT	2.5 μm
Al electrode thickness, h_{Al}	100 nm

3. Results and discussion

For the designed structure shown in Fig. 2, it is found that the phase velocity of the bulk quartz is less altered when the magnetic layer is thin. Selecting a thick magnetic layer is helpful to boost the frequency dispersion, however, this also increases the mass load of the SAW resonator, causing the additional insertion loss and decrease of the quality factor. Figure 3 plots the dependence of parameter S_{11} on the thickness of the magnetic layer. Herein, the thickness of the magnetic layer was altered by changing the layer number *n* of [FeCoSiB/SiO_2]$_n$ films from one to five. As can be seen, the bare SAW resonator has a center frequency of 314.967 MHz and a Bode-*Q* factor of 7221. Upon increasing the layer number from zero to three, the resonance frequency gradually shifts towards the lower frequency side down to 289.414 MHz. Meanwhile, the Bode-*Q* factor also decreases down to 606 when increasing the layer number to three. For the MSAW resonator with five layers of FeCoSiB, it further decreases to 288, indicating either too heavy the mass load or severe insertion loss. Therefore, the MSAW resonator with three layers of FeCoSiB, i.e., [FeCoSiB/SiO_2]$_3$, was selected in the followed magneto-acoustic response studies.

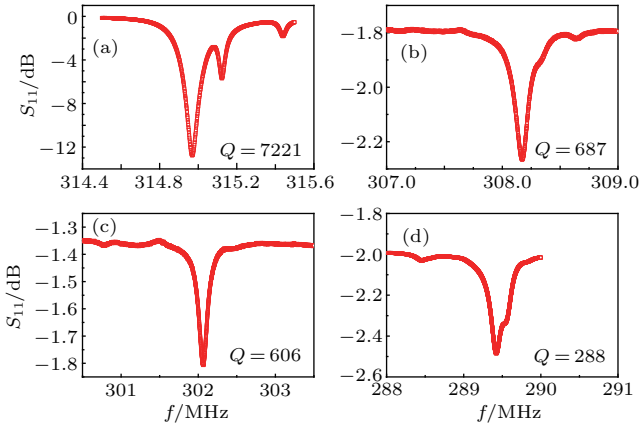


Fig. 3. Thickness dependence of the S_{11} parameter of the MSAW resonators with [FeCoSiB (160 nm)/SiO_2 (10 nm)]$_3$ films on the measured frequency, (a) bare resonator, (b) $n = 1$, (c) $n = 3$, and (d) $n = 5$.

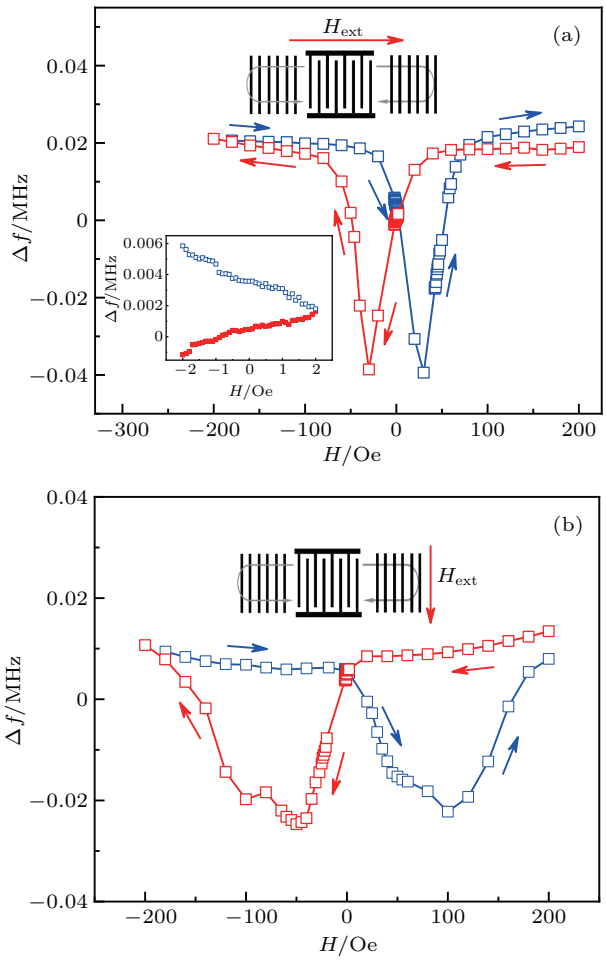


Fig. 4. The resonance frequency shift of MSAW-A as a function of the external magnetic field along (a) the SAW propagation direction and (b) the IDTs fingers.

Figure 4 shows the resonance frequency shift (Δf_R) of the MSAW-A as a function of the applied magnetic field (H). Butterfly-like Δf_R–H curves are seen in both Figs. 4(a) and 4(b), suggesting a hysteresis behavior of the ΔE effect due to the random distributed magnetic domains.[32] The f_R is lowest at ± 30 Oe in Fig. 4(a), however, the lowest f_R is obtained at about -50 Oe in Fig. 4(b), suggesting that the easy magnetization axis of the FeCoSiB film lies along the in-plane direction parallel to the SAW propagation direction due to the shape anisotropy (length 3 mm, width 0.11 mm). The maximum frequency shifts (Δf_R) are 61 kHz and 33 kHz in Figs. 4(a) and 4(b), respectively. The working point at -1.0 Oe in the inset of Fig. 4(a) has the greatest change in E or f_R per magnetic field, and therefore the largest magnetic sensitivity $\mathrm{d}f_R/\mathrm{d}H$ of 3670 Hz/Oe. In addition, when the external magnetic field varies within ± 30 Oe, E will continuously decrease as H goes from positive to negative. For applied fields within ± 2 Oe, a bipolar response of the device can be thus obtained with good linearity (see the insertion of Fig. 4(a)).

Figures 5(a) and 5(b) present the measured Δf_R–H curves of the MSAW-B with the induced magnetic anisotropy parallel to the SAW propagation direction. Although a butterfly-like Δf_R–H curve is observed in Fig. 5(a) along the SAW propagation direction, one should notice that this is the induced easy axis of the magnetic multilayered film. The ΔE effect of an anisotropic film along the easy axis is seldom discussed, since the hysteresis loop is generally explained by nucleation of reverse domains and domain wall motion instead of domain rotation. In such a case, the ΔE effect along the easy axis should be very weak,[15] therefore, contributing a negligible Δf_R. However, the butterfly-like Δf_R–H curve and the maximum Δf_R about 80 kHz suggest significant contribution from domain rotation. For amorphous FeCoSiB film with near zero magnetocrystalline anisotropy, the hysteresis behavior is heavily correlated with the magnetoelastic anisotropy. Therefore, the stress state in the [FeCoSiB/SiO_2]$_3$ film plays a critical role in determining the ΔE effect. Moreover, the surface fluctuation (Fig. 2(c)) may also imprint into the FeCoSiB films and bring additional stress anisotropy competing with the induced magnetic anisotropy.[33] Both of these may cause significant angular dispersions of the magnetic moments and favor domain rotation during magnetization switching, therefore contributing to the observed ΔE effect along the easy axis in Fig. 5(a). Similar result has been reported in an MSAW resonator using Ni as electrodes with competing shape anisotropy and induced anisotropy.[22] The largest magnetic sensitivity $\mathrm{d}f_R/\mathrm{d}H$ at the working points (± 24 Oe) is about 41900 Hz/Oe, as highlighted in Fig. 5(a).

Figure 5(b) shows the Δf_R–H curves of the MSAW-B upon applying an external magnetic field along the IDT fingers. Surprisingly, a loop-like Δf_R–H curve is seen in Fig. 5(b), which represents two bistable nonvolatile Young's moduli never reported in the literature. In addition, one of the branches in blue has relatively low $\mathrm{d}f_R/\mathrm{d}H$ less than 80 Hz/Oe upon sweeping the external field from 0 to 41 Oe. Therefore, if selecting a proper biasing field along the SAW propagation direction, the MSAW-B is suitable to detect the vector magnetic field.

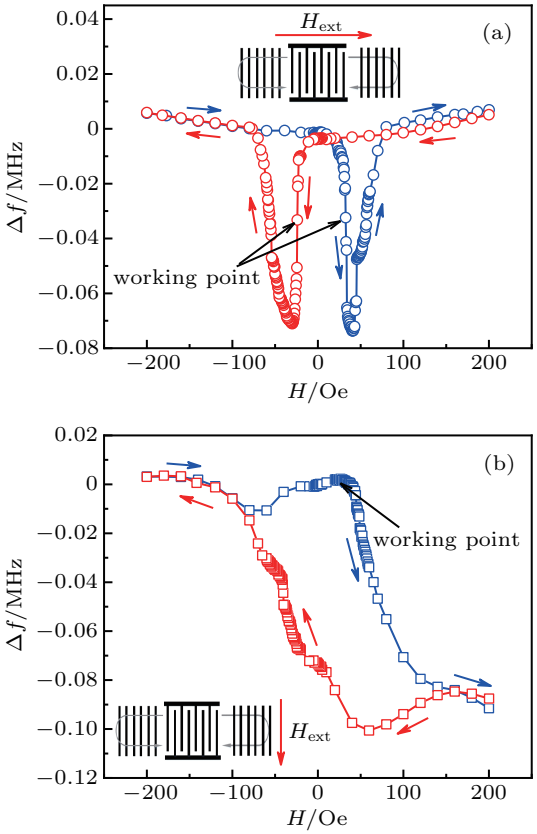


Fig. 5. The resonance frequency shift of MSAW-B as a function of the external magnetic field along (a) the SAW propagation direction and (b) the IDTs fingers.

Figure 6 presents the measured Δf_R–H curves of the MSAW-C with the induced magnetic anisotropy along the fingers of IDTs. Again, a loop-like Δf_R–H curve is seen in Fig. 6(a) upon applying a magnetic field along the SAW propagation direction (i.e., the induced hard axis). Figure 6(b) shows the Δf_R–H curves of the MSAW-C upon applying an external magnetic field along the IDT fingers. A reversible f_R–H curve is seen in Fig. 6(b) with two lowest resonance frequencies upon sweeping H field in the range of $\pm$215 Oe, which can be attributed to the ΔE effect. This behavior is typical for magnetostrictive films along the hard axis and has been well explained by Ludwig and Quandt.[15] The Young's modulus exhibits its minimum in the magnetic field where the magnetostrictive susceptibility is maximal. However, again notice that this is the induced easy axis of our magnetic multilayered film.

In order to investigate the mechanism of the loop-like curve along the hard axis and the reversible curve along the easy axis in Fig. 6, we extended the external magnetic field range to $\pm$500 Oe, and the measurement results are shown in Fig. 7. In contrast to Fig. 6(a), there are two lowest resonance frequencies in Fig. 7(a) upon sweeping the H field: the weaker one seems to come from reversible domain rotation, and the other sharp drop of f_R observed on the reverse field side strongly indicates irreversible domain rotation. The anisotropic field is as high as 400 Oe, much higher than the field induced anisotropy in Fig. 1(a). Meanwhile, the two lowest resonance frequencies in Fig. 6(b) become quite asymmetric upon increasing sweeping field to $\pm$500 Oe in Fig. 7(b), suggesting (i) the decreased contribution from the reversible domain rotation to the total ΔE effect for $\Delta f_R < 0$, and (ii) nonnegligible contribution from the irreversible rotation of the magnetic inhomogeneities and/or the out-of-plane magnetic moments[21] for $\Delta f_R > 0$. The observed resonance frequency shift in Fig. 7(b) can be attributed to the angular dispersions of the easy axis due to the competition between the induced magnetic anisotropy and the shape anisotropy. The similar phenomena have been widely reported in patterned magnetic strips with a large length over width ratio.[34] Applying higher external field triggers more irreversible domain rotation, therefore contributing to the observed enhanced ΔE effect along the easy axis.

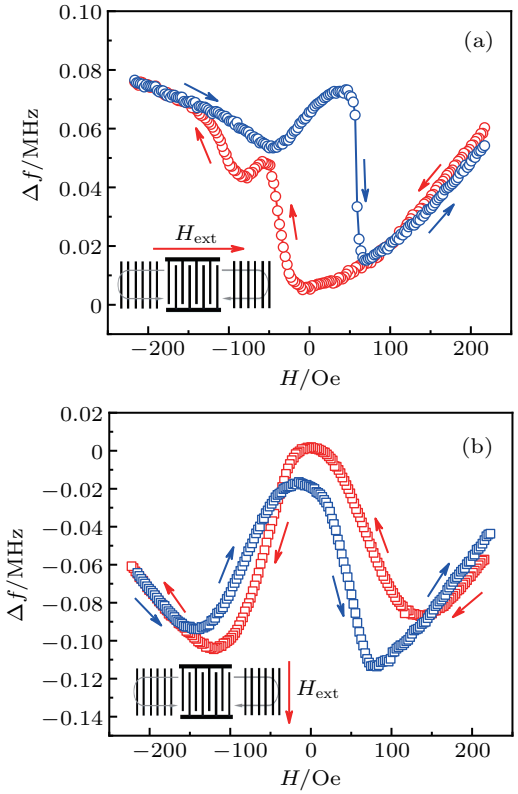


Fig. 6. The resonance frequency shift of MSAW-C as a function of the external magnetic field along (a) the SAW propagation direction and (b) the IDTs fingers.

Assuming that the magnetic moments are pre-aligned on the negative field side in Fig. 6(a), one can find that the Young's modulus first decreases upon sweeping the H field from +215 Oe (much less than the anisotropic field) to 0 Oe, and then increases upon sweeping the field from 0 Oe to −57 Oe, due to the trigger of the irreversible domain rotation first. Applying H field higher than −57 Oe triggers reversible domain rotation and slightly decrease of E. However, sweeping the H field from −215 Oe to +215 Oe triggers both reversible and irreversible domain rotations near −46 Oe and

+55 Oe sequentially, which is very like the blue branch in Fig. 7(a). Therefore, we believe that the loop-like Δf_R–H is originated from the hysteresis of the magnetoelastic properties (λ and ΔE), and can be observed as far as the sweeping field is larger than the coercivity but smaller than the anisotropic field. This explanation can also be applied to Fig. 5(b). However, for a soft magnetostrictive film with only induced magnetic anisotropy and very small coercivity, this loop-like Δf_R–H may become unconspicuous due to the suppressed contribution from the irreversible domain rotation.

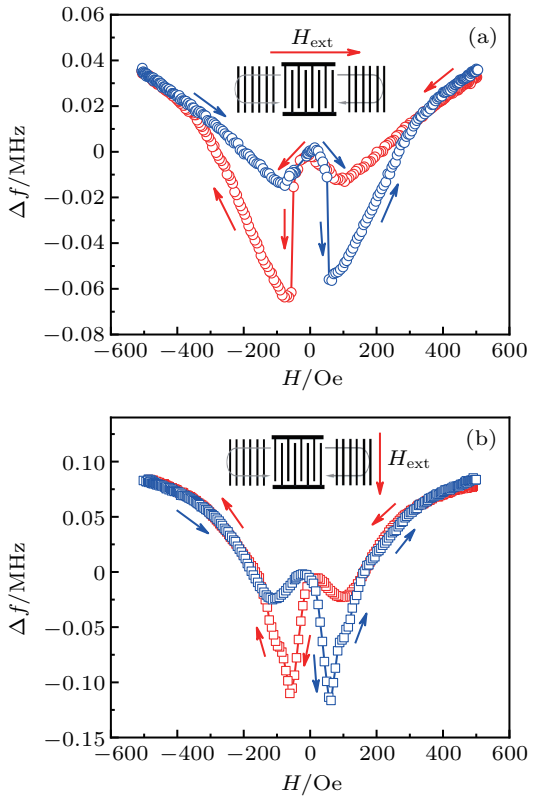


Fig. 7. The resonance frequency shift of MSAW-C as a function of the external magnetic field in a broad range from −500 Oe to +500 Oe along (a) the SAW propagation direction and (b) the IDTs fingers.

4. Conclusion and perspectives

In summary, magnetic SAW resonators have been fabricated by stacking multilayered FeCoSiB films on the top of IDTs. It is found that the resonance frequency of the MSAW resonator without induced anisotropy exhibits a butterfly-like dependence on the external field along both the SAW propagation direction and the IDTs fingers, therefore, enabling bipolar detection of magnetic field smaller than its coercive field. Distinct butterfly-like and loop-like Δf_R–H curves can be obtained by introducing magnetic anisotropy to the $[FeCoSiB/SiO_2]_n$ multilayer, which can be employed as a useful strategy to design vector magnetic field sensors.

References

[1] Nan C W, Bichurin M, Dong S, Viehland D and Srinivasan G 2008 *J. Appl. Phys.* **103** 031101
[2] Hu J M, Chen L Q and Nan C W 2016 *Adv. Mater.* **28** 15
[3] Cheng J H, Wang Y G and Dan E 2015 *Chin. Phys. Lett.* **32** 17503
[4] Dong S, Zhai J, Bai F, Li J, Viehland D and Lograsso T A 2005 *J. Appl. Phys.* **97** 103902
[5] Dong S, Zhai J, Bai F, Li J F and Viehland D 2005 *Appl. Phys. Lett.* **87** 062502
[6] Dong S, Zhai J, Xing Z, Li J F and Viehland D 2005 *Appl. Phys. Lett.* **86** 102901
[7] Wang Y, Gray D, Berry D, Gao J, Li M, Li J and Viehland D 2011 *Adv. Mater.* **23** 4111
[8] Chu Z, Shi H, Shi W, Liu G, Wu J, Yang J and Dong S 2017 *Adv. Mater.* **29** 1606022
[9] Lage E, Kirchhof C, Hrkac V, Kienle L, Jahns R, Knöchel R, Quandt E and Meyners D 2012 *Nat. Mater.* **11** 523
[10] Kirchhof C, Krantz M, Teliban I, Jahns R, Marauska S, Wagner B, Knöchel R, Gerken M, Meyners D and Quandt E 2013 *Appl. Phys. Lett.* **102** 232905
[11] Hayes P, Klug M J, Toxværd S, Durdaut P, Schell V, Teplyuk A, Burdin D, Winkler A, Weser R and Fetisov Y 2019 *Sci. Rep.* **9** 1
[12] Viehland D, Wuttig M, McCord J and Quandt E 2018 *MRS Bull.* **43** 834
[13] Ou-Yang J, Liu X, Zhou H, Zou Z, Yang Y, Li J, Zhang Y, Zhu B, Chen S and Yang X 2018 *J. Phys. D: Appl. Phys.* **51** 324005
[14] Jiles D 1995 *J. J. Phys. D: Appl. Phys.* **28** 1537
[15] Ludwig A and Quandt E 2002 *IEEE Tran. Magn.* **38** 2829
[16] Jahns R, Zabel S, Marauska S, Gojdka B, Wagner B, Knöchel R, Adelung R and Faupel F 2014 *Appl. Phys. Lett.* **105** 052414
[17] Zabel S, Kirchhof C, Yarar E, Meyners D, Quandt E and Faupel F 2015 *Appl. Phys. Lett.* **107** 152402
[18] Zabel S, Reermann J, Fichtner S, Kirchhof C, Quandt E, Wagner B, Schmidt G and Faupel F 2016 *Appl. Phys. Lett.* **108** 222401
[19] Kadota M and Ito S 2012 *Jpn. J. Appl. Phys.* **51** 07GC21
[20] Zhou H, Talbi A, Tiercelin N and Bou Matar O 2014 *Appl. Phys. Lett.* **104** 114101
[21] Elhosni M, Elmazria O, Petit-Watelot S, Bouvot L, Zhgoon S, Talbi A, Hehn M, Aissa K A, Hage-Ali S and Lacour D 2016 *Sens. Actuators A: Phys.* **240** 41
[22] Polewczyk V, Dumesnil K, Lacour D, Moutaouekkil M, Mjahed H, Tiercelin N, Watelot S P, Mishra H, Dusch Y and Hage-Ali S 2017 *Phys. Rev. Appl.* **8** 024001
[23] Wang W, Jia Y, Xue X, Liang Y and Du Z 2018 *Smart Mater. Struct.* **27** 105040
[24] Liu X, Tong B, Ou-Yang J, Yang X, Chen S, Zhang Y and Zhu B 2018 *Appl. Phys. Lett.* **113** 082402
[25] Li M, Matyushov A, Dong C, Chen H, Lin H, Nan T, Qian Z, Rinaldi M, Lin Y and Sun N X 2017 *Appl. Phys. Lett.* **110** 143510
[26] Nan T, Lin H, Gao Y, Matyushov A, Yu G, Chen H, Sun N, Wei S, Wang Z and Li M 2017 *Nat. Commun.* **8** 1
[27] Kittmann A, Durdaut P, Zabel S, Reermann J, Schmalz J, Spetzler B, Meyners D, Sun N X, McCord J and Gerken M 2018 *Sci. Rep.* **8** 1
[28] Li W, Buford B, Jander A and Dhagat P 2014 *IEEE Tran. Magn.* **50** 3100704
[29] Edrington W, Singh U, Dominguez M, Alexander J, Nepal R and Adenwalla S 2018 *Appl. Phys. Lett.* **112** 052402
[30] Wen D, Bai F, Wang Y, Zhong Z and Zhang Z 2013 *J. Appl. Phys.* **113** 17A309
[31] Wang Y, Wang L, Zhang H, Zhong Z, Peng D, Ye F and Bai F 2016 *J. Alloys Comp.* **667** 229
[32] Wiegert R F and Levy M 1988 *J. Appl. Phys.* **64** 5411
[33] Tang J, Ma B, Zhang Z Z and Jin Q Y 2010 *Chin. Phys. Lett.* **27** 077502
[34] Cheng C, Davies R, Sturkcken N, Shepard K and Bailey W 2013 *J. Appl. Phys.* **113** 17A343